

Title: Effects of attention and perceptual uncertainty on cerebellar activity during visual motion perception

Authors: Oliver Baumann & Jason B. Mattingley

The University of Queensland, Queensland Brain Institute, St Lucia 4072, Australia

Correspondence should be addressed to:

Oliver Baumann
Queensland Brain Institute
The University of Queensland
St Lucia, Queensland, 4072
Australia

Ph: +61 7 3346 3305

Fax: +61 7 3346 6301

E-mail: o.baumann@uq.edu.au

Conflicts of interest

The authors declare that no financial or personal competing interests exist. This work was supported by an Australian Research Council Discovery Early Career Researcher Award (DE120100535), a UQ Foundation Research Excellence Award and a UQ Early Career Researcher Grant to OB. JBM was supported by an Australian Research Council Australian Laureate Fellowship (FL110100103).

Abstract

Recent clinical and neuroimaging studies have revealed that the human cerebellum plays a role in visual motion perception, but the nature of its contribution to this function is not understood. Some reports suggest that the cerebellum might facilitate motion perception by aiding attentive tracking of visual objects. Others have identified a particular role for the cerebellum in discriminating motion signals in perceptually uncertain conditions. Here we used functional magnetic resonance imaging to determine the degree to which cerebellar involvement in visual motion perception can be explained by a role in sustained attentive tracking of moving stimuli in contrast to a role in visual motion discrimination. While holding the visual displays constant, we manipulated attention by having participants attend covertly to a field of random-dot motion or a colored spot at fixation. Perceptual uncertainty was manipulated by varying the percentage of signal dots contained within the random-dot arrays. We found that attention to motion under high perceptual uncertainty was associated with strong activity in left cerebellar lobules VI and VII. By contrast, attending to motion under low perceptual uncertainty did not cause differential activation in the cerebellum. We found no evidence to support the suggestion that the cerebellum is involved in simple attentive tracking of salient moving objects. Instead, our results indicate that specific subregions of the cerebellum are involved in facilitating the detection and discrimination of task-relevant moving objects under conditions of high perceptual uncertainty. We conclude that the cerebellum aids motion perception under conditions of high perceptual demand.

Keywords: cerebellum, fMRI, perception, attention, motion, uncertainty

Effects of attention and perceptual uncertainty on cerebellar activity during visual motion perception

The human cerebellum has a widely acknowledged role in a range of motor functions. Recently, however, it has become clear that the cerebellum also contributes to purely sensory functions [1,2]. Damage to the cerebellum causes deficits in complex perceptual tasks, but leaves elementary sensory functions intact [3]. In particular, individuals with cerebellar damage are often impaired in the detection and discrimination of visual motion signals in noise [4,5]. On the basis of these and other observations concerning visual motion processing, it has been proposed that the cerebellum interacts with dorsal-visual stream processes [2], increasing the efficiency of visual motion acquisition, especially under conditions of high sensory demand [6,7,8].

We recently provided direct evidence for the cerebellar “sensory acquisition hypothesis”, by identifying a set of cerebellar regions in humans that are selectively active during discrimination of both visual and auditory motion stimuli under perceptually demanding situations (i.e. short stimulus duration and low-signal to noise levels; [9]). However, a number of human brain imaging studies indicate that cerebellar activity during motion perception might not be due to bottom-up perceptual demands, but could instead reflect the “top-down” (voluntary) allocation of attention to motion signals [10-13]. For example, Kellermann and colleagues [13] used fMRI to measure cerebellar neural activity during a task in which participants viewed a salient moving-bar stimulus. The participants were

asked to either detect slight changes in the velocity of the bars or to simply passively observe the stimulus. It was found that the condition, which required active processing of the moving stimulus, led to significantly higher activity in crus I of the cerebellum. This and other similar findings [10-12] pose the question whether cerebellar activity during tasks, which require attention to motion, reflects “top-down” (voluntary) allocation of attention (i.e. covert motion tracking) or are due to the specific perceptual demands posed by the tasks employed.

The aim of the current study was to determine the degree to which cerebellar activity during visual motion perception can be explained by a role in aiding attentive tracking of visual motion, in contrast to a role in facilitating visual motion discrimination under levels of high perceptual uncertainty. Using fMRI, we monitored neural activity in the cerebellum while participants engaged in a task, which required them to identify and covertly monitor a directional visual motion signal in noise. The stimuli were random-dot kinematograms containing a central stationary fixation spot whose color alternated periodically. While holding the visual displays constant, we manipulated attention by having participants attend covertly to the dot motion or the colored spot at fixation. Perceptual uncertainty was manipulated by varying the percentage of coherently moving dots contained within the random-dot arrays. Increased cerebellar activity during attention to motion under high perceptual certainty relative to the color-monitoring task would indicate an involvement in sustained attentive tracking of moving stimuli. In contrast, increased cerebellar activity during attention to motion under high perceptual uncertainty would suggest an involvement in facilitating visual motion discrimination.

Methods

Participants

Twenty-two healthy participants gave informed written consent to the behavioral and brain imaging procedures, as approved by The University of Queensland Human Research Ethics Committee, and in accordance with the Helsinki Declaration of 1975. Participants' performance on the experimental tasks was assessed in the laboratory prior to imaging. Four participants were excluded in this training session because they were unable to meet our strict criteria for maintaining steady fixation throughout the task, leaving 18 individuals to participate in the fMRI experiment. The participants' ages ranged from 19 to 26 years (mean age = 21.9, SD = 2.1 years). Twelve of the participants were female; all were right-handed.

Pre-scan training and eye movement assessment

As noted above, participants were trained and assessed in the psychophysical laboratory prior to imaging to ensure that they were able to perform the visual motion identification task and to maintain central fixation during the experiment. First, the participants were screened to determine whether they were able to detect coherent visual motion at signal-to-noise levels used in the experiment. For this the participants were shown a series of random-dot kinematograms (5-s each) containing 0%, 7.5%, 15%, 30%, 50% or 100% coherent motion (see below for a detailed description of the visual stimuli) and were asked to indicate by vocal response whether they detected the coherently moving dots. The stimuli were presented in a staircase-like procedure, starting with the 100% stimulus

and reversing at the 0% stimulus, which was repeated twice. This initial assessment indicated that all participants were able to comfortably detect motion coherence levels of 15% and above. Subsequently, participants undertook two, 10-minute blocks (40 trials each) of the experimental task, while eye movements were recorded using an Eyelink 1000 Gazetracker (SR Research Ltd., Mississauga, Ontario, Canada) to ensure fixation compliance. The sampling frequency of the eye-tracker signal was 1000 Hz, the spatial resolution was 0.05°, and the accuracy was $\pm 0.125^\circ$. The eye-recording system was calibrated individually for each participant, to determine the exact deviation from central fixation. The eye tracker recording software was used to monitor the participants' fixation behavior, and we provided immediate verbal feedback regarding their fixation performance. Participants were informed if their eye movements deviated more than $\pm 0.3^\circ$ from the central fixation spot. During the second block of the training session, all participants not excluded due to poor performance in the first block were able to maintain constant and reliable fixation under all experimental conditions. We also conducted statistical tests to determine whether the average maximum deviation and average number of eye blinks differed across the attention manipulation and for the different signal levels in the dot-motion stimuli. There were no significant differences for any of these comparisons (paired t-tests, threshold $p = 0.05$).

Visual Stimulation

The stimuli were digital movies created with Matlab (Version 7.9). The stimuli consisted of a fixation spot (0.4°) and 400 sparse gray background dots (0.4° of visual angle) on a black background. The stationary fixation spot was displayed centrally and its color

alternated periodically (0.2Hz) between green and yellow. The background dots moved along random trajectories, creating a random-dot kinematogram. Three levels of motion coherence (0%, 15% and 30%; see Animations 1-3 in Supplemental Material) were presented. The zero-coherent motion displays constituted the *motion detection* condition. As outlined below, participants were instructed that a coherent signal would always be present in the display, but that it would sometimes be difficult to detect. The 30%-coherent motion displays constituted the *motion tracking condition*, since the pre-scan training indicated that the threshold for coherent motion detection was $\leq 15\%$ for all participants, indicating that the 30% motion stimulus was sufficiently salient to be readily discerned from noise. The purpose of the 15%-coherent motion condition was to provide trials of intermediate difficulty between the 0% and 30% displays, and thereby to increase participants' motivation to search for the signal in the 0% condition. Coherent dots moved along the horizontal axis with a sinusoidal velocity profile (0.2 Hz), and with a maximum speed at the center of the display of 12.6° per second. The speed of the random-dot trajectories was distributed over the same range and had the same mean velocity as the coherent dots. The half-life of each dot (coherent or random) was one second, after which it was replaced by another dot with a new speed and direction. These transition periods were randomized over time, such that a steady migration of dots from random to coherent, and vice versa, occurred. The direction changes of the coherent dots and the color changes of the fixation spot were out of phase, so that changes in one dimension never predicted changes in the other.

Task

The participants' task was to attend covertly to the moving dots and monitor for periods of motion coherence, or to attend to the central spot and monitor for color changes. Each trial was preceded by a visual cue to indicate the upcoming task. Both the moving dots and the central spot were present throughout the trial. To monitor participants' compliance with the task instructions, they had to indicate, at offset of the stimulus, either the last direction of the motion (left or right) or the last color of the central spot (green or yellow). The displays were presented for 4.7, 8.5, 11.2 or 16 seconds, after which participants had 2 seconds to press one of two buttons (using their right index finger) indicating their response. The durations of the stimulation periods were varied to ensure that participants could not strategically attend to just the last few seconds of the trial. As noted above, participants were not informed that there would be trials with no directional motion signal (0% coherence). Instead, they were told that the signal would occasionally be below their perceptual threshold, and that in these instances they should make their best guess as to the direction of motion immediately prior to stimulus offset. Participants were reminded to maintain fixation centrally during the experiment, and to avoid blinking during stimulus presentations. Each experimental run contained 72 trials, yielding 12 trials per condition. There were three experimental runs per participant, yielding 216 trials in total (36 per condition). The temporal design of the stimulus sequence was optimized using the program optseq2 [14]. All aspects of stimulus delivery and response recording were controlled using Presentation software (Version 14.3, Neurobehavioral Systems, Inc., Burnaby, BC, Canada).

MRI acquisition

Brain images were acquired on a 3T MR scanner (Trio; Siemens, Erlangen, Germany) with a 32-channel head coil. For the functional data thirty-five axial slices (slice thickness, 3 mm; interslice gap, 1.05mm) were acquired in a descending order, using a gradient echo echo-planar T2*-sensitive sequence (repetition time, 2.19 s; echo time, 30 ms; flip angle, 90°; matrix, 64 x 64; field of view, 210 x 210 mm; voxel size, 3.3 × 3.3 × 3.0 mm). Geometric distortions in the EPI images caused by magnetic field inhomogeneities were corrected using a point-spread mapping approach [15,16]. We also acquired a T1-weighted structural MPRAGE scan. A liquid crystal display projector back-projected the stimuli onto a screen positioned at the head of the participants in the end of the scanner gantry. Participants lay on their backs within the bore of the magnet and viewed the stimuli via a mirror that reflected the images displayed on the screen. To minimize head movement, all participants were stabilized with tightly packed foam padding surrounding the head. Because physiological variables are known to influence the BOLD response, particularly in the cerebellum [17-21], we recorded cardiac and respiration rate during the functional runs. Heart rate was recorded at 50 Hz using the pulse oximetry system integrated with the Siemens scanner (Trio; Siemens, Erlangen, Germany). Respiration was recorded at 50 Hz using the Siemens pneumatic compression belt (Siemens, Erlangen, Germany).

Image processing and statistical analysis of fMRI data

Image processing and statistical analyses were performed using SPM8 (Wellcome Department of Imaging Neuroscience, UCL, London, UK). Functional data volumes were

slice-time corrected and realigned to the first volume. A T2*-weighted mean of the images was co-registered with the corresponding anatomical T1-weighted image from the same individual. The individual T1-image was used to derive the transformation parameters for the stereotaxic space and to create an individual binary mask to exclude areas that were not part of the cerebellum, using the spatially unbiased infratentorial template (SUIT, Version 2.53) for the cerebellum and the associated normalization procedure [22,23]. The transformation parameters and the mask were then applied to the individual co-registered EPI images. The voxel size for the normalized images was 2 mm³. The binary mask and the resulting images were manually inspected and, if necessary, manually corrected using MRICron (MRICron, <http://www.sph.sc.edu/comd/rorden/mricron>) to ensure optimal segmentation. Images were then smoothed with an 8-mm full-width half maximum (FWHM) isotropic Gaussian kernel. Analyses using the general linear model [24] were conducted after applying high-pass filtering (cut-off: 128 s). To account for physiological noise we used the Physiological Log Extraction for Modeling toolbox [21] to compute models of respiratory and cardiac noise, which were included in the general linear model as regressors. The respiratory variance and response function was generated as by described by Birn et al. [19], and the heart-rate variance and response function was generated according to Chang et al [20]. We further included the 6 head motion regressors into the model (x, y, z, pitch, roll, yaw) to account for movement artifacts.

In an event-related design analysis, responses during the stimulation periods were modeled as boxcar functions convolved with a hemodynamic response function (HRF)

separately for the 6 conditions. We modeled the exact duration of each individual stimulation period (i.e. 4.7, 8.5, 11.2 or 16 seconds) in SPM so that the height and duration of the corresponding HRFs were scaled accordingly for every trial. The relevant conditions were contrasted using t-statistics, generating the contrast images for second level evaluation. These images were analyzed at the group level with SPM8 using two planned t-tests to test for effects of *motion tracking*, as well as *motion detection*. First, to test whether the cerebellum was active during simple attentive tracking of a salient supra-threshold motion signal, we conducted a planned comparison of the condition requiring attention to a strong coherent motion signal with the corresponding color-control condition (Attend motion (30%) > Attend color (30%)). Second, to test whether the cerebellum was active during the motion detection task, we compared the condition with no coherent motion signal to the condition with the corresponding color-control condition (Attend motion (0%) > Attend color (0%)). Brain regions were counted as active if they surpassed a statistical threshold of $p = 0.05$ (corrected for multiple comparisons), on either a voxel- or cluster-level (height threshold $p = 0.001$). A probabilistic atlas of the cerebellum [23,25] and MRICron (MRICron, <http://www.sph.sc.edu/comd/rorden/mricron>) was used to identify cerebellar anatomical locations. The locations of cortical regions were derived from the AAL atlas [26].

Results

Behavioral data

The average accuracy rates for the fMRI study were very high in both conditions in which a coherent motion signal was present; the participants responded correctly in

90.1% of the trials with 15% motion coherence and in 95.1% of the trials with 30% motion coherence (see Figure 1a). As expected, the accuracy in the color-control task was also very high, averaging 93.2% across all three conditions. To verify that the motion color conditions were comparable in their general level of difficulty, we conducted a repeated-measures, 2 x 2 ANOVA with the factors Task (Motion or Color) and Coherence (15% or 30%). There was no significant main effect of Task ($F(1,17) = 1.443$, $p = 0.246$), but there was a significant main effect for Coherence ($F(1,17) = 17.670$, $p = 0.01$) and a significant interaction between Task and Coherence ($F(1,17) = 41.818$, $p < 0.001$). Post-hoc paired t-tests revealed that accuracy in the motion condition was lower than in the control condition for 15%-coherent motion displays ($t(17) = 3.102$, $p = 0.006$), but not for 30%-coherent motion displays ($t(17) = 0.546$, $p = 0.592$), indicating that the lower signal-to-noise levels in the 15% condition negatively affected the participants' coherent motion detection performance. Post-hoc paired t-tests revealed that Coherence had no effect in the control task ($t(17) = 0.101$, $p = 0.921$). This indicates that the level of motion coherence did not affect participants' performance in the control condition. In the motion condition with no signal (0% signal strength) the proportion of "left" responses was 50.8% (SE = 2.64%), which is not significantly different from 50% (t-test, threshold $p = 0.412$).

The response times (RT), measured from stimulus offset, show that participants needed on average less than 800 ms to indicate their decision (see Figure 1b). It is also evident that in the motion condition with zero-coherence, participants took around 100 ms longer to make their responses than in the 15% and 30% conditions. To test these observations

we conducted a repeated-measures, 2 x 3 ANOVA with the factors Task (Motion or Color) and Coherence (0%, 15% or 30%). There was no significant effect of Task ($F(1,17) = 3.183, p = 0.092$), but there was a significant main effect of Coherence ($F(1,17) = 27.547, p < 0.001$) and a significant interaction between Task and Coherence ($F(1,17) = 61.953, p < 0.001$). A series of post-hoc, pairwise comparisons between the different coherence levels, conducted separately for each attention condition, confirmed that the mean RT in the zero-coherence condition was significantly greater than that in all other conditions ($p < 0.001$). There were no other reliable differences between conditions. This result suggests that participants needed extra time to make a decision when there was no motion signal on which to base their judgment.

fMRI data

The aim of this study was to determine the degree to which cerebellar activity during visual motion perception can be explained by a role in sustained attentional motion tracking, in contrast to a role in facilitating visual motion discrimination under levels of high perceptual uncertainty. First, to test the degree to which the cerebellum is involved in sustained attentive tracking of moving objects we compared the level of BOLD signal associated with attention to a salient supra-threshold motion signal (i.e. no perceptual uncertainty) with the corresponding color-control condition (Attend motion (30%) > Attend color (30%)). This contrast failed to reveal any significant difference in activation within the cerebellum ($p > 0.001$, uncorrected). Second, to test whether the cerebellum was active during the motion discrimination task, we compared the condition with no coherent motion signal to the condition with the corresponding color-control condition

(Attend motion (0%) > Attend color (0%). Using this comparison, we identified two left hemispheric activation clusters (see Figure 2a-c). The first was located at the border between hemispheric lobules VI and Crus I (-36 -44 -33, cluster size = 337). The second cluster was located at the border between paravermal lobules Crus II and VIIB (-12 -76 -45, cluster size = 279). The cerebellar lobules VI and VII are known to be involved in various cognitive and perceptual tasks [27], and are functionally connected to prefrontal, posterior parietal and visual cortices [28].

To further explore the specificity of the relationship between cerebellar activity in these regions and perceptual uncertainty, we extracted parameter estimates from the peak voxels for contrasts involving different levels of visual motion coherence (see Figure 3). These results show that attention to motion under high visual uncertainty (zero-coherence) led to reliable levels of cerebellar activity. While the condition with the 15%-coherent motion displays appeared to show a weak but similar trend, attentive tracking of a salient supra-threshold motion signal (30% coherence) did not evoke any obvious activity in these regions. This pattern implies that these regions of the cerebellum are strongly activated while participants search for a particular motion stimulus in noise, but not when they track a salient suprathreshold motion signal.

To test whether the motion tracking task successfully activated cortical regions commonly found to be involved during attention to salient visual motion, we also performed exploratory whole-brain analyses using the comparison of the condition requiring attention to a salient supra-threshold motion signal with the corresponding

color-control condition (Attend motion (30%) > Attend color (30%)). This comparison revealed significant activity in several key regions ($p = 0.05$, corrected for multiple comparisons, on either a voxel- or cluster-level (height threshold $p = 0.001$; see Figure 2d and Table 1) commonly associated with attention to visual motion [13,29,30], including the superior parietal lobule (SPL; Brodmann area 7), the inferior frontal gyrus (IFG; Brodmann area 44) and early visual cortex (Brodmann areas 18 and 19).

Discussion

Recent clinical and neuroimaging studies strongly suggest a cerebellar contribution to the processing of visual motion signals [3]. However, two hypotheses can be proposed for its particular role. Cerebellar activity during tasks, which require attention to motion, could be either reflective of a role in aiding “top-down” (voluntary) allocation of attention (i.e. covert motion tracking) [10-13] or in supporting the detection and discrimination of sensory signals in perceptually demanding situations [4,9,31,32].

We used fMRI to measure cerebellar activity across changes in voluntary attentional allocation and different levels of perceptual uncertainty. Attention to a salient, supra-threshold motion signal did not lead to noticeably higher activity in the cerebellum compared to a control task. By contrast, attention to motion under high levels of perceptual uncertainty led to increased activity in two left hemispheric regions located in cerebellar lobule VI and Crus I, as well as lobule VIIIB and Crus II. Our results therefore support the notion that the cerebellum facilitates the detection and discrimination of moving objects under conditions of high perceptual uncertainty [4,9], but are inconsistent

with the idea that the cerebellum is crucial for sustained attentive tracking of salient motion stimuli [10-13].

Our results indicate that previous reports of cerebellar activity during visual motion perception were not reflective of simple sustained attention to motion, but were rather due to the specific perceptual and/or cognitive demands posed by the tasks employed. A possible explanation for the cerebellum's role in visual motion perception is that it monitors and adjusts sensory data acquisition processes in cortical visual areas, resulting in increased sensitivity to visual motion signals [6-8]. Under conditions of severely degraded or ambiguous visual input, these cerebellar regulatory processes could be engaged to facilitate the detection of moving targets. This model of cerebellar involvement in sensory perception is further corroborated by neural connectivity studies in humans and other animals, which suggest that the cerebellar regions identified in our study are connected with areas of the cerebral cortex [3,28,33,34] involved in visual motion detection and perception [35,36]. More specifically, cerebellar lobule VI is functionally connected with motion sensitive visual area MT [28], whereas the left cerebellar lobules VIIA (crus I and crus II) and VIIB maintain connections with prefrontal and posterior parietal cortices [28,33]. Through these connections the cerebellum could provide a regulatory sensory support function, optimizing visual motion detection whenever bottom-up motion signals from the visual cortex cannot be readily distinguished from noise.

It is important to emphasize that the cerebellar regions identified in our study are likely to be involved in perceptual functions beyond the visual modality, since activity in these regions has also been found during auditory tasks [9,32,37]. As with vision, the cerebellum is particularly active in auditory tasks that are perceptually complex or demanding. For example, Petacchi et al [32] found that cerebellar activity was positively correlated with the degree of perceptual uncertainty in a sequential pitch discrimination task. The involvement of the lateral cerebellum in visual as well as auditory tasks fits with the suggestion that the cerebellar hemispheres have a crucial multimodal [38] or supramodal [39] function in sensory processing, consistent with the finding that inputs from different areas of the cerebral cortex converge on common areas within the neocerebellum.

The cerebellum also has a well-known role in the control of eye movements (e.g. [40-42], and it has been shown that the execution of both smooth pursuit eye movements [43] and saccades [44] leads to increased BOLD signals in the cerebellum. For this reason, we took care to minimize possible contributions from unwanted eye movements. Our participants underwent extensive fixation training prior to the MRI session, and only those participants who were able to maintain fixation to a strict criterion were subsequently scanned. We therefore believe that it is unlikely that the cerebellar activation patterns identified in this study are attributable to unexpected eye movements.

It is also noteworthy that our task elicited only left hemisphere activity within the cerebellum. This finding dovetails with numerous clinical and imaging studies of

cerebellar function, which have indicated that non-verbal processes tend to be left-lateralized, whereas language processes are more right-lateralized (see [27] for an overview). Our findings are therefore unlikely to reflect differences in covert verbalization. Similarly, our results are unlikely to be explained by differences in response mapping demands. Participants responded using their right index finger, which is represented in the right cerebellar hemisphere [45], and we observed activations that were exclusively within the left cerebellar hemisphere. Finally, we took care to correct our data for the influence of heart rate and breathing, to control for unwanted physiological artifacts that are a particular issue for studies of cerebellar activity [46].

Conclusion

In summary, we have shown that the left cerebellar lobules VI and VII are active during visual motion perception, but only under conditions of high perceptual uncertainty. Our results suggest that the cerebellum contributes to the process of visual motion detection and discrimination, but that it does not play a central role in the voluntary sustained allocation of attention to motion. We propose that cerebellar activity under high perceptual uncertainty reflects the operation of regulatory processes that coordinate the acquisition of sensory data [6-8] and facilitate the discrimination of moving targets from noise.

Acknowledgments

This work was supported by an Australian Research Council Discovery Early Career Researcher Award (DE120100535), a UQ Foundation Research Excellence Award and a

UQ Early Career Researcher Grant to OB. JBM was supported by an Australian Research Council Australian Laureate Fellowship (FL110100103).

References

1. Paulin MG. The role of the cerebellum on motor control and perception. *Brain Behav Evol.* 1993;41:39-50.
2. Schmahmann JD. The cerebrocerebellar system: anatomic substrates of the cerebellar contribution to cognition and emotion. *Int Rev Psychiatry.* 2001;13:247-60.
3. Bastian AJ. Moving, sensing and learning with cerebellar damage. *Curr Opin Neurobiol.* 2011;21:596-601.
4. Thier P, Haarmeier T, Treue S, Barash S. Absence of a common functional denominator of visual disturbances in cerebellar disease. *Brain.* 1999;122:2133-46.
5. Jokisch D, Troje NF, Koch B, Schwarz M, Daum I. Differential involvement of the cerebellum in biological and coherent motion perception. *Eur J Neurosci.* 2005;21:3439-46.
6. Bower JM. Control of sensory data acquisition. In: Schmahmann JD, editor. *The cerebellum and cognition.* San Diego: Academic; 2007. pp. 489–513.

7. Bower JM. The organization of cerebellar cortical circuitry revisited: implications for function. *Ann N Y Acad Sci.* 2002;978:135-55.
8. Bower JM. Computational structure of the cerebellar molecular layer. In: Manto M, Gruol D, Schmahmann J, Koibuchi N, Rossi F, editors. *Handbook of the Cerebellum and Cerebellar Disorders.* New York: Springer; 2013. pp. 1359-1380.
9. Baumann O, Mattingley JB. Scaling of neural responses to visual and auditory motion in the human cerebellum. *J Neurosci.* 2010;30:4489-95.
10. Jovicich J, Peters RJ, Koch C, Braun J, Chang L, Ernst T. Brain areas specific for attentional load in a motion-tracking task. *J Cogn Neurosci.* 2001;13:1048-58.
11. Thakral PP, Slotnick SD. The role of parietal cortex during sustained visual spatial attention. *Brain Res.* 2009;1402:157-66.
12. Jahn G, Wendt J, Lotze M, Papenmeier F, Huff M. Brain activation during spatial updating and attentive tracking of moving targets. *Brain Cogn.* 2012;78:105-13.
13. Kellermann T, Regenbogen C, De Vos M, Mößnang C, Finkelmeyer A, Habel U. Effective connectivity of the human cerebellum during visual attention. *J Neurosci.* 2012;32:11453-60.

14. Dale AM. Optimal experimental design for event-related fMRI. *Hum Brain Mapp.* 1999;8:109-14.
15. Zeng H, Constable RT. Image distortion correction in EPI: comparison of field mapping with point spread function mapping. *Magn Reson Med.* 2002;48:137-46.
16. Zaitsev M, Steinhoff S, Shah NJ. Error reduction and parameter optimization of the TAPIR method for fast T1 mapping. *Magn Reson Med.* 2003;49:1121-32.
17. Glover GH, Li TQ, Ress D. Image-based method for retrospective correction of physiological motion effects in fMRI: RETROICOR. *Magn Reson Med.* 2000;44:162-7.
18. Shmueli K, Van Gelderen P, de Zwart JA, Horovitz SG, Fukunaga M, Jansma JM, Duyn JH. Low-frequency fluctuations in the cardiac rate as a source of variance in the resting-state fMRI BOLD signal. *Neuroimage.* 2007;8:306-20.
19. Birn RM, Smith MA, Jones TB, Bandettini PA. The respiration response function: the temporal dynamics of fMRI signal fluctuations related to changes in respiration. *Neuroimage.* 2008; 40:644-54.
20. Chang C, Cunningham JP, Glover GH. Influence of heart rate on the BOLD signal: the cardiac response function. *Neuroimage.* 2009;44:857-69.

21. Verstynen TD, Deshpande V. Using pulse oximetry to account for high and low frequency physiological artifacts in the BOLD signal. *Neuroimage*. 2011;55:1633-44.
22. Diedrichsen J. A spatially unbiased atlas template of the human cerebellum. *Neuroimage*. 2006;33:127-38.
23. Diedrichsen J, Maderwald S, Küper M, Thürling M, Rabe K, Gizewski ER, Ladd ME, Timmann D. Imaging the deep cerebellar nuclei: a probabilistic atlas and normalization procedure. *Neuroimage*. 2011;54:1786-94.
24. Friston KJ, Holmes AP, Worsley KJ, Poline JP, Frith CD, Frackowiak RSJ. Statistical parametric maps in functional imaging: a general linear approach. *Hum Brain Mapp*. 1995;2:189-210.
25. Diedrichsen J, Balsters JH, Flavell J, Cussans E., Ramnani N. A probabilistic atlas of the human cerebellum. *Neuroimage*. 2009;46:39-46.
26. Tzourio-Mazoyer N, Landeau B, Papathanassiou D, Crivello F, Etard O, Delcroix N, et al. Automated anatomical labeling of activations in SPM using a macroscopic anatomical parcellation of the MNI MRI single subject brain. *Neuroimage*. 2002;15:273-89.

27. Stoodley CJ, Valera EM, Schmahmann JD. Functional topography of the cerebellum for motor and cognitive tasks: an fMRI study. *Neuroimage*. 2012; 59:1560-70
28. O'Reilly JX, Beckmann CF, Tomassini V, Ramnani N, Johansen-Berg H. Distinct and overlapping functional zones in the cerebellum defined by resting state functional connectivity. *Cereb Cortex*. 2010;20:953-65.
29. Büchel C, Josephs O, Rees G, Turner R, Frith CD, Friston KJ. The functional anatomy of attention to visual motion. A functional MRI study. *Brain*. 1998;121:1281-94.
30. Culham JC, Brandt SA, Cavanagh P, Kanwisher NG, Dale AM, Tootell RB. Cortical fMRI activation produced by attentive tracking of moving targets. *J Neurophysiol*. 1998;80:2657-70.
31. Parsons LM, Petacchi A, Schmahmann JD, Bower JM. Pitch discrimination in cerebellar patients: evidence for a sensory deficit. *Brain Res*. 2009;15:84-96.
32. Petacchi A, Kaernbach C, Ratnam R, Bower JM. Increased activation of the human cerebellum during pitch discrimination: a positron emission tomography (PET) study. *Hear Res*. 2011;282:35-48.

33. Habas C, Kamdar N, Nguyen D, Prater K, Beckmann CF, Menon V, Greicius MD. Distinct cerebellar contributions to intrinsic connectivity networks. *J Neurosci.* 2009;29:8586-94.
34. Buckner RL, Krienen FM, Castellanos A, Diaz JC, Yeo BT. The organization of the human cerebellum estimated by intrinsic functional connectivity. *J Neurophysiol.* 2011;106:2322-245.
35. Shulman GL, McAvoy MP, Cowan MC, Astafiev SV, Tansy AP, d'Avossa G, Corbetta M. Quantitative analysis of attention and detection signals during visual search. *J Neurophysiol.* 2003;90:3384-97.
36. Shulman GL, Ollinger JM, Linenweber M, Petersen SE, Corbetta M. Multiple neural correlates of detection in the human brain. *Proc Natl Acad Sci U S A.* 2001;98:313-8.
37. Petacchi A, Laird AR, Fox PT, Bower JM. Cerebellum and auditory function: an ALE meta-analysis of functional neuroimaging studies. *Hum Brain Mapp.* 2005; 25:118-228.
38. Lewis JW. Audio-visual perception of everyday natural objects – hemodynamic studies in humans. In: Naumer J, Kaiser J, editors. *Multisensory object perception in the primate brain.* New York: Springer; 2010.

39. Schmahmann JD. From movement to thought: anatomic substrates of the cerebellar contribution to cognitive processing. *Hum Brain Mapp.* 1996;4:174-198.
40. Baumann O, Ziemus B, Luerding R, Schuierer G, Bogdahn U, Greenlee MW. Differences in cortical activation during smooth pursuit and saccadic eye movements following cerebellar lesions. *Exp Brain Res.* 2007;181:237-47
41. Leigh JR, Zee DS. *The Neurology of Eye Movements*, Oxford University Press. New York; 2006.
42. Lynch JC, Tian JR. Cortico-cortical networks and cortico-subcortical loops for the higher control of eye movements. *Prog Brain Res.* 2006;151:461-501.
43. Tanabe J, Tregellas J, Miller D, Ross RG, Freedman R. Brain activation during smooth-pursuit eye movements. *Neuroimage.* 2002;17:1315-24.
44. Dieterich M, Bucher SF, Seelos KC, Brandt T. Cerebellar activation during optokinetic stimulation and saccades. *Neurology.* 2000;54:148-55.
45. Grodd W, Hülsmann E, Lotze M, Wildgruber D, Erb M. Sensorimotor mapping of the human cerebellum: fMRI evidence of somatotopic organization. *Hum Brain Mapp.* 2001;13:55-73.

46. Schlerf J, Ivry RB, Diedrichsen J. Encoding of sensory prediction errors in the human cerebellum. *J Neurosci.* 2012;32:4504-11.

47. Luft AR, Skalej M, Welte D, Kolb R, Burk K, Schulz JB, Klockgether T, Voigt K. A new semiautomated, three-dimensional technique allowing precise quantification of total and regional cerebellar volume using MRI. *Magn Reson Med.* 1998;40:143-151.

48. Schmahmann JD, Doyon J, Toga AW, Petrides M, Evans AC. MRI atlas of the human cerebellum. San Diego: Academic; 2000.

Tables

Region	Hemisphere	Brodmann area	MNI coordinates			t-values / Z-values of maxima	Cluster size in number of voxels
			x	y	z		
Effects of attentive motion tracking (low perceptual uncertainty)							
(Attention to 30% coherent motion > Attention to color)							
Cortex							
LingG/MOG/MTG	L	18/19/37	-22	-76	-6	10.37/5.75	1962
LinG/MOG/MTG	R	18/19/37	18	-84	-4	9.93/5.64	2968
PrecG/MFG/SFG	R	6	28	-6	54	9.11/5.42	450
SPL	L	7	-24	-58	60	9.10/5.42	464
SFG/PcecG	L	6	-24	-8	52	9.02/5.39	420
SPL	R	7	20	-62	60	8.14/5.13	642

IFG	R	44	60	14	24	7.27/4.84	150
Effects of motion detection (high perceptual uncertainty)							
(Attention to 0% coherent motion > Attention to color)							
Cerebellum							
Hemispheric lobule VI/Crus I	L	-	-12	-76	-45	6.72/4.69	337
Paravermal lobule VIIIB/Crus II	L	-	-36	-44	-33	6.60/4.65	279

Table 1 Summary of fMRI findings for all contrasts

Spatial coordinates, anatomical locations and cluster-size of the local maxima in the group analysis, showing significant activations ($p \leq 0.05$, corrected for multiple comparisons). Abbreviations: IFG = inferior frontal gyrus, L = left hemisphere, LinG = lingual gyrus, MFG = middle frontal gyrus, MOG = middle occipital gyrus, MTG = middle temporal gyrus, PrecG = precentral gyrus, SFG = superior frontal gyrus, SPL= superior parietal lobule, R = right hemisphere. Sagittal divisions were defined according to [47]; vermis: $-10 \text{ mm} \leq x \leq +10 \text{ mm}$; left and right paravermal region: $-24 \text{ mm} \leq x < -10 \text{ mm}$, $+10 \text{ mm} < x \leq +24 \text{ mm}$; left and right lateral hemispheres: $x < -24 \text{ mm}$, $x > +24 \text{ mm}$).

Figures

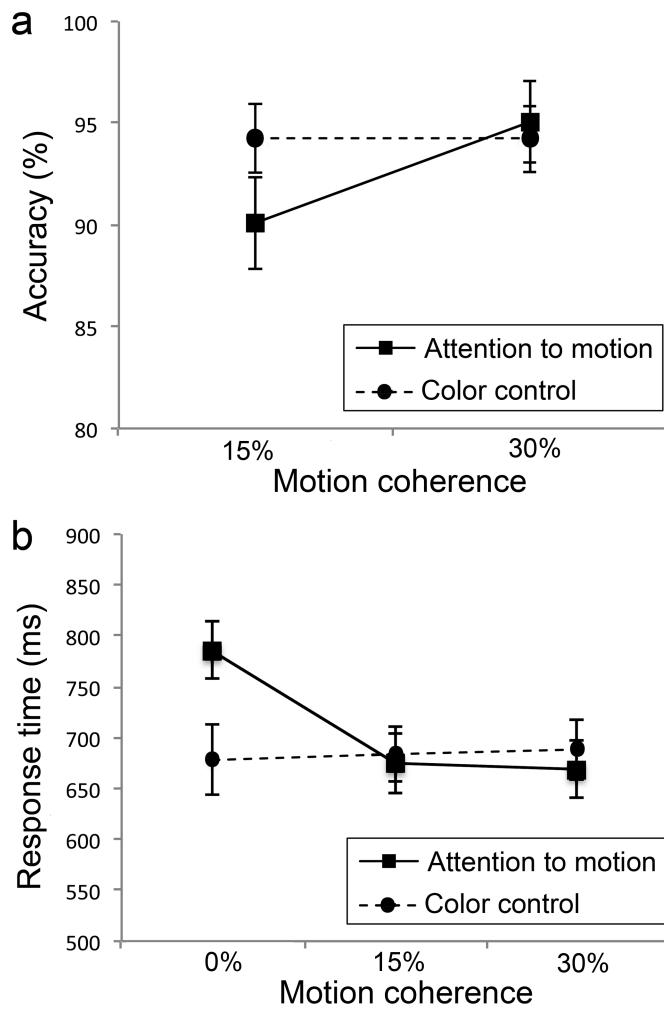


Fig 1. Mean accuracy rates and response times (± 1 SE) for the two experimental tasks under different levels of visual motion coherence.

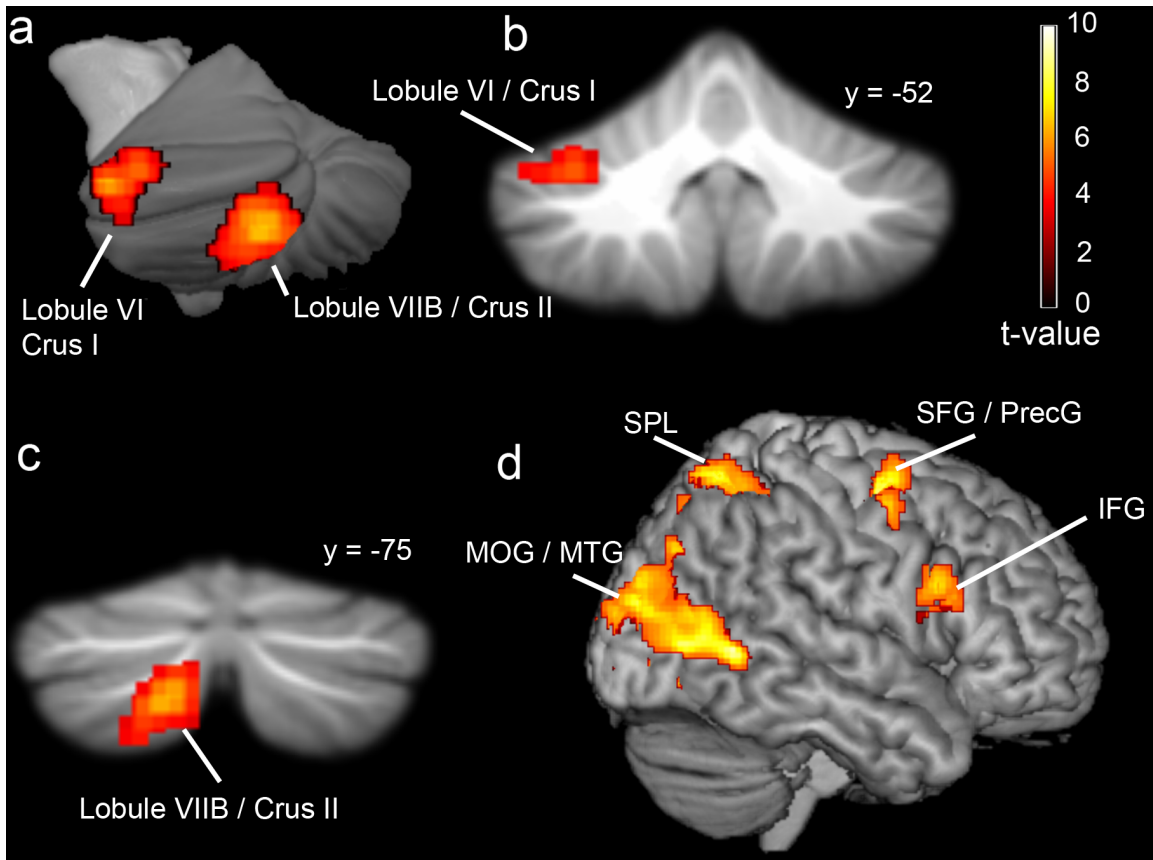


Fig 2. MR anatomical templates depicting mean BOLD activity from the random-effects analysis comparing effects of top-down attentional demands and perceptual uncertainty during visual motion perception. The locations of cerebellar anatomical regions (nomenclature according to [48]) were derived using the probabilistic atlas of the cerebellum by Diedrichsen et al [22,23]. The locations of cortical regions were derived from the AAL atlas [26]. **a-c**, Cerebellar effects of motion detection (high perceptual uncertainty; Attend motion (0%) > Attend color). **d**, Cortical effects of attention to a salient superthreshold motion signal (high perceptual certainty; Attend motion (30%) > Attend color).

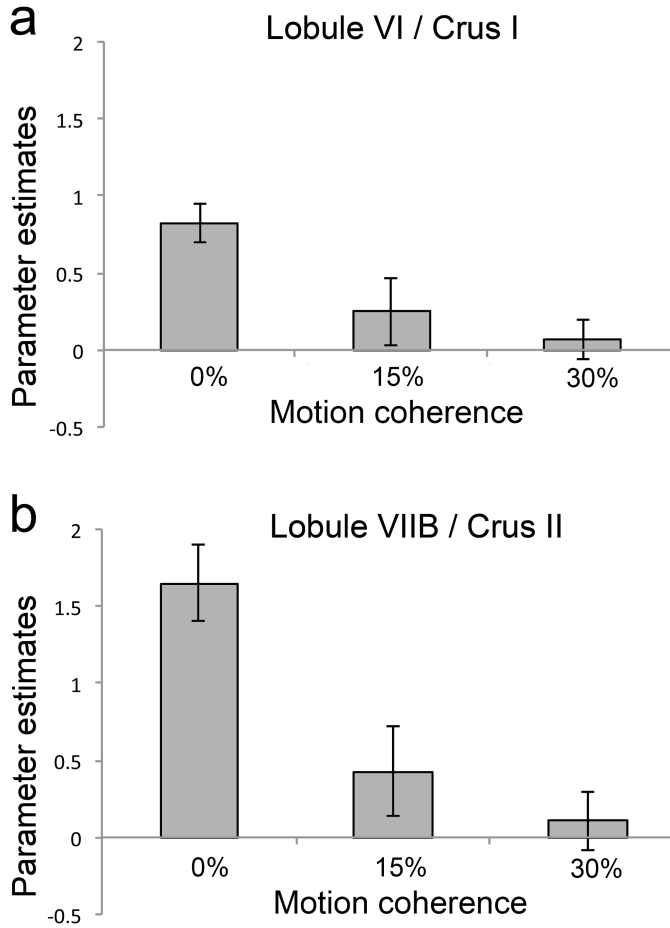


Fig 3. Parameter estimates (beta values, $\pm 1SE$) for effects of attending to motion (Attend motion > Attend color) under three different levels of motion coherence. Peak voxels are derived from the random-effects analysis probing neural activity associated with motion detection (high perceptual uncertainty; Attend motion (0%) > Attend color).